

RESEARCH ARTICLE

Preparation of Lysine-Coated Magnetic Fe_2O_3 Nanoparticles and Influence on Viability of A549 Lung Cancer Cells

Yu-Hua Ma¹, Hai-Ying Peng¹, Rui-Xia Yang², Fang Ni^{2*}

Abstract

Objective: To explore the effect of lysine-coated oxide magnetic nanoparticles (Lys@MNPs) on viability and apoptosis of A549 lung cancer cells. **Methods:** Transmission electron microscopy (TEM), vibrating sample magnetometer (VSM) and Zeta potentiometric analyzer were employed to characterize Lys@MNPs. Then Lys@MNPs and lung cancer A549 cells were co-cultured to study the effect of Lys@MNPs on cell viability and apoptosis. The pathway of Lys@MNPs entering A549 cells was detected by TEM and cell imaging by 1.5 T MRI. **Results:** Lys@MNPs were 10.2 nm in grain diameter, characterized by small size, positive charge, and superparamagnetism. Under low-dose concentration of Lys@MNPs (< 40 $\mu\text{g}/\text{mL}$), the survival rate of A549 cells was decreased but remained higher than 95% while under high-dose concentration (100 $\mu\text{g}/\text{mL}$), the survival rate was still higher than 80%, which suggested Lys@MNPs had limited influence on the viability of A549 cells, with good biocompatibility and no induction of apoptosis. Moreover, high affinity for cytomembranes, was demonstrated presenting good imaging effects. **Conclusion:** Lys@MNPs can be regarded as a good MRI negative contrast agents, with promising prospects in biomedicine.

Keywords: Oxide magnetic nanoparticle - lysine - lung cancer cells - magnetic resonance imaging - cell viability

Asian Pac J Cancer Prev, **15** (20), 8981-8985

Introduction

Magnetic nanoparticles (MNPs), which have unique properties of superparamagnetism, alternating current magnetic heating, magnetic quantum tunnel effect and good biocompatibility, is widely applied in the field of biomedical domain such as magnetic resonance imaging (MRI) contrast agent, immunoassay, magnetic heat treatment, drug release and cell sorting (Fang et al., 2012; Sterenczak et al., 2012; Rosen et al., 2012; Barick et al., 2014; Bogart et al., 2014; Singh et al., 2014; Wabler et al., 2014; Weis et al., 2014).

In order to achieve better diagnosis and treatment effect, MNPs are modified and constructed to deeply study its biological effect according to different application requirements (Basuki et al., 2013; Lee et al., 2014; Riaz et al., 2014; Sun et al., 2014). MNPs shows great potential in MRI contrast agent, however, there is a limitation in application of MNPs achieving cell imaging in the current study. For example, efficient uptake nanoparticles, effective gathering in the lesions, imaging signal amplification and the improvement of imaging quality are needed to be further studied (Bakhru et al., 2012; Laesen et al., 2012; Huang et al., 2013; Huang et al., 2013; Weis et al., 2014).

Small molecule lysine is one of the important components of protein, which can't synthesize itself, but

it is one of eight very necessary amino acids in human body, and selected as coated material widely used in food and pharmaceutical industries. Small molecule lysine has amino and hydroxyl groups, characterized by no toxicity, no antigenicity, good biocompatibility, biodegradability, promotion of the growth and development, improvement of drug efficacy and so on. This study employed lysine to modify oxide magnetic nanoparticles to explore its application in high quality imaging and its influence on cell viability and apoptosis of A549 lung cancer cells.

Materials and Methods

Preparation and surface characterization of lysine coated magnetic nanoparticles

Lysine coated magnetic iron oxide nanoparticles ($\gamma\text{-Fe}_2\text{O}_3$) was prepared using coprecipitation method according to the literature (Ma et al., 2003) and expressed as Lys@MNPs. The specific modification methods are as follows: Proper amount of lysine was dissolved in a small amount of distilled water and after fully dissolved, rapidly added with a certain amount of magnetic liquid (molar ratio of lysine/iron element is 1: 20) through full ultrasonic dispersion. The total reaction system (100 mL) was mechanically stirred for 4 h under the protection of nitrogen, washed by distilled water repeatedly for removing free lysine molecules after magnetic separation

¹Department of Clinical Laboratory Medicine, Linyi People's Hospital, Linyi, Shandong, ²Department of Laboratory Medicine, The First Affiliated Hospital of Nanjing Medical University, Nanjing, Jiangsu, China *For correspondence: yunerniyunerni@163.com

and preserved at 4 °C after constant volume.

Transmission electron microscopy (TEM, JEM-200CX, JEOL, Japan) was used for describing morphological characterization of Lys@MNPs. The method was shown below: Magnetic nanoparticles liquid was dripped into 300-mesh copper net and determined after natural drying. The magnetic properties of the sample were described using vibrating sample magnetometer (VSM 7407, Lakeshore, USA). Properties of the surface charge under physiological conditions (Ph 7.4) were described using Zeta potentiometric analyzer.

Cell culture

A549 lung cancer cells were purchased from Shanghai Cell Institute, Chinese Academy of Sciences (CAS). RPMI 1640 culture containing 10% FCS, which was used for cell culture in 5% CO₂ incubator at 37 °C, was changed every two days. Cells were inoculated into 6-well or 96-well plate after when they were fusion to about 90% and cell growth was in a good state and was used when fusion to about 80%.

Detection of cell viability by MTT

A549 cells with concentration of 1×10⁴ cell/mL were inoculated into 96-well plate, 100 μL/well for 24 h incubation, then added with Lys@MNPs culture solution with different final concentrations of 0, 10, 20, 40, 60, 80 and 100 μg/mL for 24 h co-incubation and washed by PBS after removing culture solution. After MTT solution (20 μL) was added into each well for 4 h incubation in the incubator, 200 μL Dimethyl sulfoxide (DMSO) was added and shaken for 30 min. Biv-tek instruments inc was used to select 590nm in wave length for calculating optional density (OD). Blank control was designed for color comparisons. Cell survival rate (%) = $\frac{OD_{\text{measured value}}}{OD_{\text{blank control}}}$

Detection of cell apoptosis by FCM

Blank cells and marked Lys@MNPs cells were collected, washed two times with PBS and then suspended by 50 μL buffer solution. The suspension was added with 5 μL Annexin V-FITC at room temperature away from light for 10 min, mixed with 10 μL prodium iodide (PI) at room temperature, kept in dark place for 5 min, and after washed by PBS, added with 300 μL buffer solution for resuspended cells which was detected using flow cytometry (FCM).

Detection of cell section by TEM

After A549 cells and Lys@MNPs were co-incubated for 6 hours and digested by trypsin, the collected cells were centrifuged to remove the supernatant, and resuspended by adding with PBS, then centrifuged twice, fixed by 2.5% glutaraldehyde solution at 4 °C for 1 h and then by 1% osmium tetroxide at room temperature for 1 h, and washed by PBS three times, 5 min each time. Ethanol dehydration, epoxy resin embedding and routine ultrathin sections were done (70nm). Sections were observed by TED (HITACHI-600, Japan) after was transferred into 300-mesh cooper net and dyed by uranyl acetate.

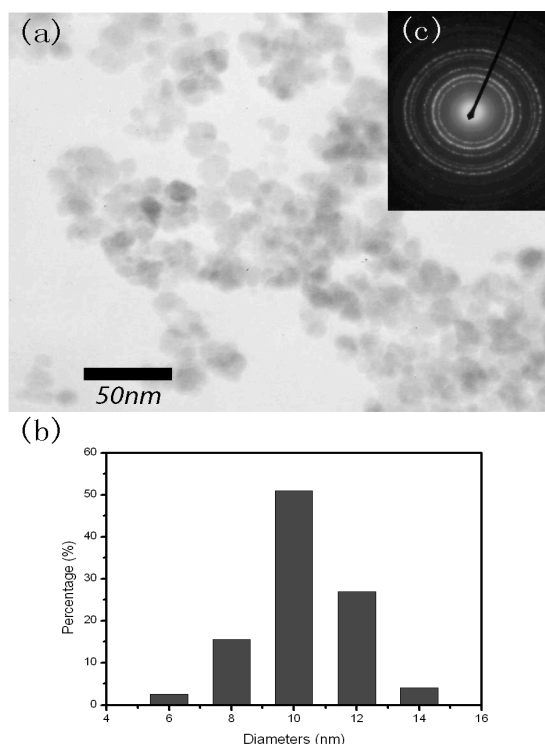


Figure 1. (a) TEM of Lys@MNPs; (b) Statistical Distribution Histogram of Grain Diameter; and (c) Electron Diffraction Image

Analysis of magnetic resonance imaging (MRI)

After 0.25% trypsin digestion, the collected Lys@MNPs-labeled and unlabeled cells were counted, centrifuged and suspended in Eppendof containing 0.5 mL 1% agarose. MRI of cell suspension was analyzed by 1.5 T MR instrument (Philip Company, Eclipse type) and the parameters included inner diameter of surface loop (12.7 cm), field of vision (FOV, 14 cm×14 cm), number of excitation (NEX, 2~4), layer thickness 2 mm, scan matrix 384×256 and signal strength region of interest (ROI, 20 mm²). Imaging sequence: (1) Spin echo (SE) impulse sequence: T1WI, repetition time (TR) 500.0 ms and echo time (TE) 17.9 ms. (2) Fast spin echo (FSE) impulse sequence: T2WI, TR 4 000 ms or 4 063 ms, TE 108 ms, echo train length 16 or 30. (3) Gradient echo (GrE) impulse sequence: T2WI, TR 620 ms, TE 15.7 ms, flip angle 35°. The known concentration of Lys@MNPs was diluted at equal ratio and suspended in Eppendof tube containing 0.5 mL 1% agarose and 0.5 mL distilled water was set as control group.

Statistical data analysis

The result in the experiment was expressed by $\bar{x} \pm s$ and SPSS software package was used for data analysis.

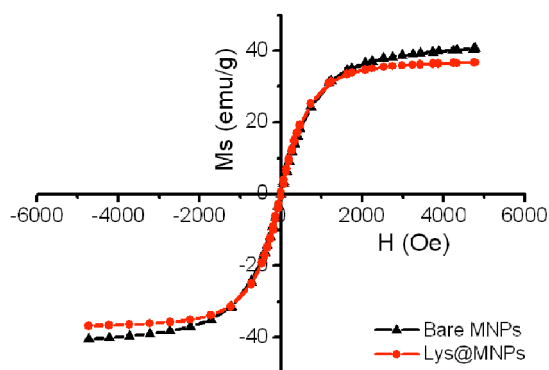
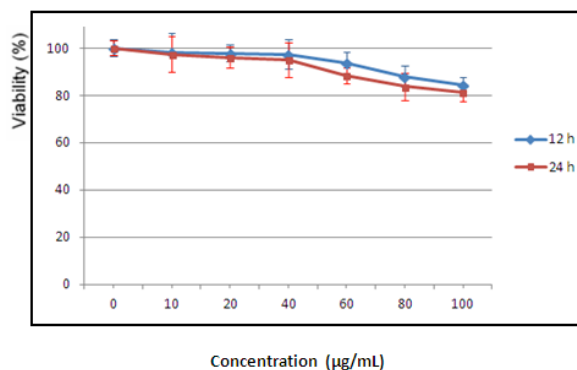
Results

Property characterization of Lys@MNPs

Morphology of Lys@MNPs was characterized by approximate sphere, evenly distributed particle, average grain diameter 10.2 nm (Figure 1a and 1b). Figure 1c was Electron diffraction image, from which nano-particles is

Table 1. The Viability of A549 Cells at the Different Concentrations and Incubation Time ($\bar{x}\pm s$)

Lys@MNPs ($\mu\text{g/mL}$)	A549 cells viability (%)	
	12 h	24 h
0	100.0 \pm 3.6	100.0 \pm 3.1
10	98.1 \pm 8.4	97.4 \pm 7.6
20	97.9 \pm 3.4	96.1 \pm 4.3
40	97.3 \pm 6.2	95.1 \pm 7.3
60	93.7 \pm 4.7	88.5 \pm 3.4
80	88.1 \pm 4.3	83.7 \pm 5.6
100	84.4 \pm 3.1	81.3 \pm 3.7

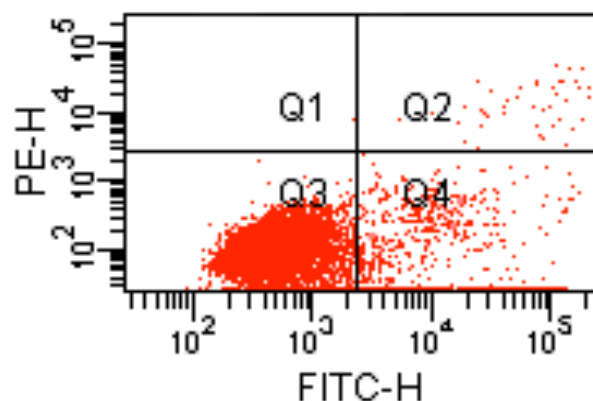
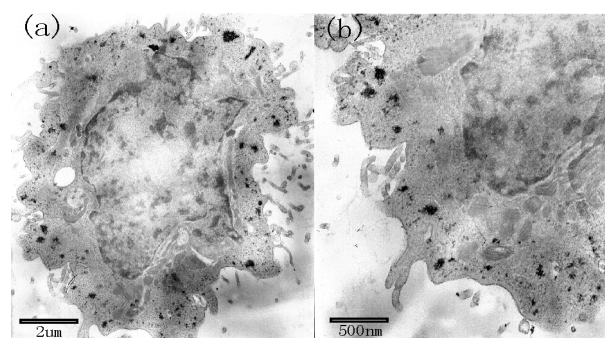
**Figure 2. Magnetic Hysteresis Chart of Lys@MNPs****Figure 3. The viability of A549 Cells at the Different Concentrations and Incubation Time**

$\gamma\text{-Fe}_2\text{O}_3$ nanoparticles of cubic spinel structure.

Saturation magnetization (M_s) and coercive force (H) are the important technical parameters of characterizing magnetism. From Figure 2, saturation magnetization of bare MNPs was 40.58 emu/g while Lys@MNPs reduced to 36.72 emu/g because nonmagnetic substance on nanoparticle surface increased after lysine modification. Coercive force and residual magnetism tended to be zero, showing they were superparamagnetism. When saturation magnetization was up to 3 000 Oe, it tended to be saturated, paralleled with abscissa axis, showing Lys@MNPs had superparamagnetism, connecting with lysine molecules on nanoparticle surface. Further exploration of surface charge characteristic under physiological condition of pH 7.4 revealed bare MNPs and Lys@MNPs were different in electrical property, -316 mV and 4.8 mV, respectively, because there were positively charged amidogen on MNPs surface after lysine modification.

Cell viability and apoptosis of A549 in vitro

After Lys@MNPs and A549 cells co-cultured for 24 h,

**Figure 4. The Effect of Lys@MNPs on The Apoptosis of Cells****Figure 5. TEM Image of Lys@MNPs and A549 Cells After 12 h Co-incubation**

the viability of A549 cells at the different concentrations and incubation time was as shown in Table 1, showing the survival rate of A549 cells and Lys@MNPs were related in a dose-dependent manner. Under low-dose concentration of Lys@MNPs (<40 $\mu\text{g/mL}$), the survival rate decreased little but higher than 95% while under high-dose concentration (100 $\mu\text{g/mL}$), the survival rate decreased but still over 80%, which suggested Lys@MNPs had less influence on the viability of A549 cells, with good biocompatibility (Figure 3).

Meanwhile, Annexin V-FITC/PI was used to detect the effect of Lys@MNPs on the apoptosis of cells. From the results of FCM, Lys@MNPs couldn't cause the apoptosis of A549 cells when the concentration of Lys@MNPs was less than 0.1 mg/mL after 12 h incubation. Viable non-apoptotic cells in the area of Q3 took up over 90% of the total cell number, viable apoptotic cells in the area of Q4 and non-viable apoptotic and necrotic cells in the area of Q2 accounted for 8% and 0.5%, respectively, which showed Lys@MNPs had good biocompatibility and didn't cause the apoptosis of A549 cells (Figure 4).

Observation of cell section

TEM proved that the large amount of Lys@MNPs entered A549 cells, with high labeling rate. As shown in Figure 5, Lys@MNPs partially entered late endosomes or lysosomes, marked by the formation of cluster embedded in the cytoplasm but didn't appear in endoplasmic reticulum, mitochondria, golgi apparatus and nucleus.

Cell imaging

As shown in Figure 6, T2WI signal intensity was

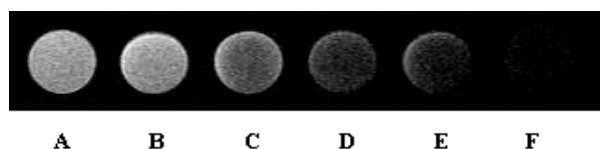


Figure 6. T₂WI MRI of Lys@MNPs and A549 Cells for 2 h Co-incubation. A and B were Distilled Water and 1×10⁵ Unlabeled Cells of Control Group; C, D, E and F were Lys@MNPs-Labeled Cells and the Cell Populations were 1×10², 1×10³, 1×10⁴ and 1×10⁵

different after the Lys@MNPs-labeled A549 cells were diluted and scanned by MRI. Control A and B were distilled water and 1×10⁵ unlabeled cells and C, D, E and F were Lys@MNPs-labeled cells and the cell populations were 1×10², 1×10³, 1×10⁴ and 1×10⁵, respectively. The signal of distilled water was the weakest. The signal of unlabeled cells of control group had no significant change. T2WI signal was enhanced with the increase of cell number after 20 μg Lys@MNPs and A549 cells for 2 h co-incubation, especially enhanced in cell number of 1×10³ and significantly enhanced in cell number of 1×10⁴. Therefore, Lys@MNPs had high affinity and detection sensitivity to A549 cells.

Discussion

The experimental treatment for lung cancer is developed quickly in China (Huang et al., 2013; Liang et al., 2013; Wang et al., 2013; Zhang et al., 2013). Oxide magnetic nanoparticles were widely applied in biomedical domain, especially in MRI contrast agent. In this study, Lys@MNPs were γ-Fe₂O₃ nanoparticle, characterized by small size, positive charge, and superparamagnetism. After co-cultured with lung cancer A549 cells, biocompatibility and image of Lys@MNPs were observed and the pathway of Lys@MNPs entering A549 cells was analyzed. The research results showed that the cell survival rate and Lys@MNPs are dose-dependent. After 12 h co-incubation of Lys@MNPs and A549 cells, the survival rate of A549 cells was over 95% under low-dose concentration (< 40 μg/mL) and over 86% under high-dose concentration (100 μg/mL). After 24 h co-incubation of Lys@MNPs and A549 cells, under low-dose concentration of Lys@MNPs (< 40 μg/mL), the survival rate decreased little but still higher than 95% while under high-dose concentration (100 μg/mL), the survival rate decreased but still over 80%, which suggested Lys@MNPs had less influence on the viability of A549 cells, with good biocompatibility, satisfying the need of biomedicine.

Lys@MNPs at low-dose concentration entered A549 cells, clustered around cytoplasm and membrane structure and didn't obviously affect the growth of cells. When Lys@MNPs increased and accumulated to a certain amount, the apoptosis was caused. From the results of FCM (Figure 4), Lys@MNPs couldn't cause the apoptosis of A549 cells when the concentration of Lys@MNPs was less than 0.1 mg/mL after 12 h incubation. When the concentration was more than 0.1 mg/mL, the broken cytomembrane was enclosed by MNPs and cells started to die and presented irregular shape, showing MNPs should be used in the proper concentration.

In this study, viable non-apoptotic cells in the area of Q3 took up over 90% of the total cell number, viable apoptotic cells in the area of Q4 and non-viable apoptotic and necrotic cells in the area of Q2 accounted for 8% and 0.5%, respectively, which showed Lys@MNPs had good biocompatibility and didn't cause the apoptosis of A549 cells.

Lysine has a large number of amidogenes which can interact with negative charge on the surface of cytomembrane (Ge et al., 2009; Ding et al., 2014). The uptakes of nanoparticles in the non-macrophage cells was mainly through absorption endocytosis, partly through clathrin-mediated endocytosis instead of passive diffusion and fluid-phase endocytosis (Gupta et al., 2005). Therefore, Lys@MNPs connected with cytomembrane through nonspecific absorption and entered cells through endocytosis.

Lys@MNPs is a negative contrast agent, because the more MNPs enter A549 cells, the stronger T2WI signal intensity and the darker the MRI. It has high affinity to cytomembrane, presenting good imaging effect. After 2 h co-incubation of Lys@MNPs and A549 cells, T2WI signal intensity is obviously enhanced with the increase of cell number, especially in cell number of 1×10³ and significantly in cell number of 1×10⁴. The result shows that Lys@MNPs is considered as a good MRI contrast agent, with the further potential application.

References

- Bakhr SH, Altioek E, Highley C, et al (2012). Enhanced cellular uptake and long-term retention of chitosan-modified iron-oxide nanoparticles for MRI-based cell tracking. *Int J Nanomed*, **7**, 4613-23.
- Basuki JS, Duong HTT, Macmillan A, et al (2013). Polymer-grafted, nonfouling, magnetic nanoparticles designed to selectively store and release molecules via ionic interactions. *macromolecules*, **46**, 7043-54.
- Barick KC, Singh S, Bahadur D, et al (2014). Carboxyl decorated Fe₃O₄ nanoparticles for MRI diagnosis and localized hyperthermia. *J Colloid Interface Sci*, **418**, 120-5.
- Bogart LK, Pourroy G, Murphy CJ, et al (2014). Nanoparticles for imaging, sensing, and therapeutic intervention. *Acs Nano*, **8**, 3107-22.
- Ding MM, Zeng X, He XL, et al (2014). Cell internalizable and intracellularly degradable cationic polyurethane micelles as a potential platform for efficient imaging and drug delivery. *Biomacromolecules*, **15**, 2896-906.
- Fang C, Kievit FM, Veisoh O, et al (2012). Fabrication of magnetic nanoparticles with controllable drug loading and release through a simple assembly approach. *J Control Release*, **162**, 233-41.
- Gupta AK, Gupta M (2005). Cytotoxicity suppression and cellular uptake enhancement of surface modified magnetic nanoparticles. *Biomaterials*, **26**, 1565-73.
- Ge YQ, Zhang Y, Xia JG, et al (2009). Effect of surface charge and agglomerate degree of magnetic iron oxide nanoparticles on KB cellular uptake in vitro. *Colloid Surface B Biointerfaces*, **73**, 294-301.
- Huang J, Wang LY, Lin R, et al (2013). Casein-coated iron oxide nanoparticles for high MRI contrast enhancement and efficient cell targeting. *ACS Appl Mater Interfaces*, **5**, 4632-9.
- Huang G, Chen HB, Dong Y, et al (2013). Superparamagnetic iron oxide nanoparticles: amplifying ROS stress to improve anticancer drug efficacy. *Theranostics*, **3**, 116-26.
- Huang XE, Tian GY, Cao J, et al (2013). Pemetrexed as a component of first-, second- and third- line chemotherapy in treating patients with metastatic lung adenocarcinoma. *Asian Pac J Cancer Prev*, **14**, 6663-7.

- Larsen EK, Nielsen T, Wittenborn T, et al (2012). Accumulation of magnetic iron oxide nanoparticles coated with variably sized polyethylene glycol in murine tumors. *Nanoscale*, **4**, 2352-61.
- Lee N, Choi Y, Lee Y, et al (2012). Water-dispersible ferrimagnetic iron oxide nanocubes with extremely high r (2) relaxivity for highly sensitive *in vivo* MRI of tumors. *Nano Lett*, **12**, 3127-31.
- Liang AL, Zhang TT, Zhou N, et al (2013). Fused polypeptide with DEF induces apoptosis of lung adenocarcinoma cells. *Asian Pac J Cancer Prev*, **14**, 7339-44.
- Ma M, Zhang Y, Yu W, et al (2003). Preparation and characterization of magnetite nanoparticles coated by amino silane. *Colloids Surf A Physicochem Eng Asp*, **212**, 219-26.
- Rosen JE, Chan L, Shieh DB, et al (2012). Iron oxide nanoparticles for targeted cancer imaging and diagnostics. *Nanomedicine*, **8**, 275-90.
- Riaz S, Bashir M, Naseem S (2014). Iron oxide nanoparticles prepared by modified co-precipitation method. *Ieee T Magn*, **50**.
- Sterenczak KA, Meier M, Glage S, et al (2012). Longitudinal MRI contrast enhanced monitoring of early tumour development with manganese chloride (MnCl₂) and superparamagnetic iron oxide nanoparticles (SPIOs) in a CT1258 based *in vivo* model of prostate cancer. *BMC Cancer*, **12**, 284.
- Singh A, Sahoo SK (2014). Magnetic nanoparticles: a novel platform for cancer theranostics. *Drug Discov Today*, **19**, 474-81.
- Sun SH (2014). Chemical synthesis of monodisperse magnetic nanoparticles for sensitive cancer detection. *J Inorg Organomet*, **P 24**, 33-8.
- Wang YL, Li B, Xu F, et al (2012). *In vitro* cell uptake of biocompatible magnetite/chitosan nanoparticles with high magnetization: a single-step synthesis approach for *in-situ*-modified magnetite by amino groups of chitosan. *J Biomater Sci Polym Ed*, **23**, 843-60.
- Weis C, Blank F, West A, et al (2014). Labeling of cancer cells with magnetic nanoparticles for magnetic resonance imaging. *Magn Reson Med*, **71**, 1896-905.
- Wabler M, Zhu WL, Hedayati M, et al (2014). Magnetic resonance imaging contrast of iron oxide nanoparticles developed for hyperthermia is dominated by iron content. *Int J Hyperthermia*, **30**, 192-200.